# Power Control-Based Multi-User Li-Fi Using A Compound Eye Transmitter

Tezcan Cogalan*, Harald Haas* and Erdal Panayirci†

*Li-Fi Research and Development Centre
Institute for Digital Communications
The University of Edinburgh
Edinburgh, EH9 3JL, UK
Email: {t.cogalan, h.haas}@ed.ac.uk

†Kadir Has University
Department of Electronics Engineering
Istanbul, 34083, Turkey
Email: {eepanay}@khas.edu.tr

***Abstract*—In visible light communications (VLC), the transmitted signal is non-negative and real valued, and these characteristics constrain the signal space and provide new challenges for waveform design in a multi-user system. In Light Fidelity (Li-Fi), a VLC technology, and similar to radio frequency (RF) systems, precoder designs can be used to serve multiple users. However, a signal shaping algorithm is required to address the non-negativity of the transmitted signal in Li-Fi. In this study, a power allocation algorithm is proposed to achieve a multi-user Li-Fi system. A compound eye transmitter consisting of several LEDs pointing in different directions is used. This means that the process of the obtaining the inverse of the channel matrix in precoder design is not required. Results show that when a $30^{\circ}$ semi-angle is used at the transmitter and the system has 4 users, the proposed transmission model can achieve $10^{-5}$ average bit error rate (BER) performance at 1 dBm average transmission power.**

## I. Introduction

Most mobile data traffic is generated by smart mobile devices in indoor environments [1]. Deploying smaller cells is becoming an important solution to enhance coverage and capacity indoors, although the limited capacity of the radio frequency (RF) spectrum remains a technical challenge. Thus, frequencies beyond 10 GHz, i.e. millimeter waves, terahertz waves and optical waves, have been proposed as an alternative to the currently used RF spectrum [2]. Light Fidelity (Li-Fi) is a proposed visible light communications (VLC) technology that is complementary for RF systems [3, 4]. In Li-Fi, light emitting diodes (LEDs) are used for signal transmission and intensity modulation (IM) is used to convey information on the instantaneous optical power of the LED. On the receiver side, photodiodes (PDs) are used to generate a photocurrent proportional to the received instantaneous optical intensity by using the direct detection (DD) technique [3]. In Li-Fi, the transmitted signal is a non-negative and real-valued signal, and the received signal is an accumulation of the received optical power intensity and hence, RF based techniques cannot be applied directly to Li-Fi systems [4–8].

In RF communications, both multiple input single output (MISO) and multiple input multiple output (MIMO) systems have been extensively researched to enhance system capacity. In multi-user systems, transmit processing techniques, such as precoding techniques, are required to mitigate both inter-cell and intra-cell interference and to improve the system and user capacity [9–11]. Recently, precoding techniques have been studied in indoor MISO and MIMO Li-Fi systems [5–8], and, due to the non-negativity of the IM signal and non-linearity effect of a LED, power allocation algorithms need to be applied as part of the precoder design.

Multi-user MISO Li-Fi systems are studied in [6, 8] when zero-forcing (ZF) based precoder and in [7] when minimum mean square error (MMSE) based precoders are used. In both studies, convex programming tools are used to design the precoder and to allocate the optical transmission power to deal with the non-negativity constraint of IM signal. In [8], the ZF based linear precoding technique is used as designed in [6], when a single-cell with multiple LEDs and multi-users with single PD MISO system is deployed. In [8], different from [6], one LED array with multiple LEDs is used as a transmitter in order to investigate the effects of the physical features of the transceiver components on the system bit error rate (BER) when users are randomly located. In [6–8], the LEDs at the transmitter are pointed downwards. Hence, when a large semi-angle is used at the transmitter, intra-cell interference increases and a multi-user system with multiple transmitters requires interference cancellation by obtaining the inverse or finding the eigenvectors of the channel matrix. When a small semi-angle is used at the transmitter, intra-cell interference and the illumination area decreases. Decreasing the illumination area means more LED fixtures are needed to give the required level of illumination. However, when the LEDs with a small semi-angle in a LED fixture are pointed in a slightly different direction, the intra-cell interference is decreased and the area and level of the illumination is unaffected. This type of LED array structure is termed a 'compound eye transmitter' or 'angle diversity transmitter', and it is not necessary to obtain the inverse or find the eigenvectors of the channel matrix to mitigate intra-cell interference. Note that the intra-cell interference is not totally cancelled by using compound eye transmitter because of the propagation nature of the light

978-1-4799-5952-5/15/$31.00 ©2015 IEEE

beams.

In this study, instead of designing a precoder by obtaining the inverse or finding the eigenvectors of the channel matrix to mitigate the interference, the advantages of the non-negativity of the transmitted signal and of the accumulation of the received optical power intensity are employed to propose a simple transmission and reception algorithms. As noted, in Li-Fi even when interference is fully mitigated by using precoders, a signal shaping algorithm is still needed. Thus, in the proposed system model, a compound eye transmitter is used to divide the illumination area into small areas, termed 'attocells' in Li-Fi cellular networks [12], and a power allocation algorithm is used to mitigate the intra-cell interference.

The paper is organized as follows. The system model is described in Section II, including the channel model employed in the proposed transmission approach. The simulation parameters and results are presented in Section III. Finally, conclusions are presented in Section IV.

## II. System Model

A single-cell multi-user optical wireless MISO system is considered. The system is equipped with a single LED array $(N_t = 1)$ which consists of multiple LEDs $(N_{t,\ell} = 1, 2, ..., L)$ at the transmitter side, and multiple users $(k = 1, 2, ..., K)$ with a single PD $(N_r = 1)$ at the receiver side. The received signal vector is shown by the conventional discrete model:

$$\mathbf{y} = r\mathbf{HP} + \mathbf{n}, \tag{1}$$

where $\mathbf{y}$ is the $(K \times 1)$ received signal vector; $r$ is the PD responsivity (optical-to-electrical conversion factor) constant; $\mathbf{H}$ is the $(K \times L)$ channel DC gain matrix; $\mathbf{P}$ is the $(L \times 1)$ DC bias vector for the LED array; and $\mathbf{n}$ is the real-valued $(K \times 1)$ noise vector with zero-mean and $\sigma_n^2$ variance. In this study, both a thermal noise due to circuit components at the receiver side and an ambient shot light noise due to surrounding light sources are taken into consideration. Thus, the noise variance $\sigma_n^2$ is:

$$\sigma_n^2 = 2er\left(P_{\text{signal},k} + P_{\text{ambient},k}\right)B + i_{\text{amp}}^2 B, \tag{2}$$

where $e$ is the electronic charge; $P_{\text{signal},k}$ is the average received power at user $k$; $B$ is the receiver bandwidth; and $P_{\text{ambient},k}$ is the received ambient light power at user $k$:

$$P_{\text{signal},k} = \mathbf{H}_k\mathbf{P}, \tag{3}$$

$$P_{\text{ambient},k} = \chi_{\text{amb}} A_{R_x} 2\pi \left(1 - \cos(\theta_k)\right), \tag{4}$$

where $\chi_{\text{amb}}$ is the photocurrent of the ambient light power; $A_{R_x}$ is the physical area of the receiver; and $\theta_k$ is the incidence angle from the transmitter to receiver $k$.

### A. Channel Model

Calculation of the channel DC gain between the transmitter and users is divided into two parts [13]. The first part is the direct path gain between the transmitter and receiver, which is termed line of sight (LOS), and the second is the reflected path, non-line of sight (NLOS), from the transmitter to a reflection point and then to the receiver. Thus, for the total channel DC gain calculation, side walls, ceiling and floor are considered as reflection points in (5):

$$\mathbf{H} = H_{\text{LOS}} + \sum_{w=1}^{W} H_{\text{NLOS},w}, \tag{5}$$

where $W$ is equal to 6 (4 side walls, ceiling and floor), and $H_{\text{LOS}}$ is:

$$H_{\text{LOS}} = \frac{(m+1)A_{R_x}G}{2\pi d_{T_x\to R_x}^2}\cos^m(\varphi_{T_x\to R_x})\cos(\theta_{T_x\to R_x})\text{rect}\left(\frac{\theta_{T_x\to R_x}}{\text{FOV}_{R_x}}\right), \tag{6}$$

where $m$ is the Lambertian order and depends on the transmitter semi-angle, $\Psi_{\frac{1}{2},T_x}$, $(m = -\ln 2/\ln(\cos(\Psi_{\frac{1}{2},T_x})))$; $G$ is the optical filter gain; $A_{R_x}$ is the area of the receiver; and $\varphi$ is the divergence angle. The symbol $A \to B$ indexes the angles from $A$ to $B$. $\text{FOV}_{R_x}$ is the field-of-view (FOV) of the receiver and the function rect gives 0 or 1 according to ratio of the incidence angle and FOV of the receiver. If the absolute value of the ratio is smaller than or equal to 1, the rect function gives 1 and otherwise, it gives 0.

Calculation of the NLOS path is also divided into two parts: transmission from the transmitter to a reflection point and from the reflection point to the receiver, as given in (7). For the calculation of the reflected paths, each reflection surface (walls) is divided into sub-areas. Firstly, LOS transmission from the transmitter to these sub-areas is calculated (8). When the sub-areas reflect the emitted light from the transmitter, they also act as a transmitter but the re-emitted light is degraded by a reflection coefficient, $\rho$, of the surface (9):

$$H_{\text{NLOS},w} = \sum_{n_w=1}^{N_w} H_{T_x\to n_w} H_{n_w\to R_x} \tag{7}$$

$$H_{T_x\to n_w} = \frac{(m+1)\Delta A_{n_w}}{2\pi d_{T_x\to n_w}^2}\cos^m(\varphi_{T_x\to n_w})\cos(\theta_{T_x\to n_w})\text{rect}\left(\frac{\theta_{T_x\to n_w}}{\text{FOV}_{n_w}}\right) \tag{8}$$

$$H_{n_w\to R_x} = \frac{\rho_w(n+1)A_{R_x}G}{2\pi d_{n_w\to R_x}^2}\cos^n(\varphi_{n_w\to R_x})\cos(\theta_{n_w\to R_x})\text{rect}\left(\frac{\theta_{n_w\to R_x}}{\text{FOV}_{R_x}}\right) \tag{9}$$

In equation (8), $\Delta A_{n_w}$ is the area of the sub-area; and in the equation (9), $n$ is the Lambertian order of the reflection surface. In general, $n$ is considered to be 1 [13].

### B. Proposed Transmission Strategy

*1) Transmitter Structure:* Existing light fixtures consist of a different number of LEDs depending on the manufacturer's design. In this study, a LED array consisting of 16 LEDs (L=16) is considered for the purpose of showing the proof of concept. As shown in Fig. 1(a), the LED array is composed of 10 LEDs on an outer circle, 5 LEDs on an inner circle and 1 LED at the center of the circle. The LEDs on the outer and inner circle are oriented $\alpha_{xz}$ and $\alpha_{xz}/2$ degree outward from the center, respectively, and the LED in the center points downwards as shown in Fig. 1(b).

The purpose of pointing the LEDs on the outer circle outwards is to increase the channel power distribution at the edge of an indoor environment. Thus, the LEDs on the inner circle, termed central LEDs for the rest of this paper, and

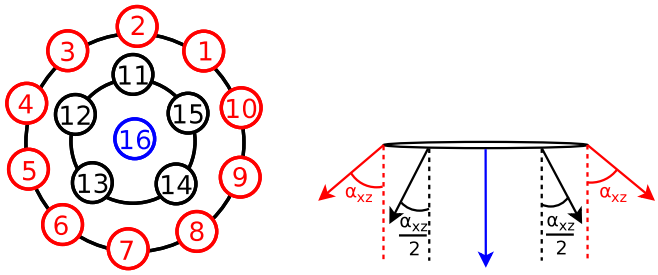


(a) Vertical view (b) Horizontal view

Fig. 1. LED array structure

LEDs located on the outer circle cover the whole indoor area equally.

*2) LED Selection Algorithm:* In the given LED array structure, each LED covers a different part of the room (for a detailed illustration, see Fig.1 in [12]). However, interference is not totally mitigated because of the propagation of the light beams. Thus, when multiple users are located at the center of the same covered area by a LED located on the outer circle, the users also receive signal from the central LEDs because of their orientation. Accordingly, a LED selection algorithm, as shown in Algorithm 1, activates all of the central LEDs, and selects only one outer LED per user according to the achieved channel DC gains.

According to the given LED selection algorithm, the new received signal $\mathbf{y}'$ is:

$$\mathbf{y}' = r\mathbf{H}' \left(P_b \mathbf{P}'\right) + \mathbf{n}, \tag{10}$$

where $\mathbf{H}'$ is the $(K \times L_{\text{act}})$ channel matrix between the users and activated LEDs; $P_b$ is the DC bias power value; and $\mathbf{P}'$ is the $(L_{\text{act}} \times 1)$ power coefficients vector of the activated LEDs.

Fig. 2 shows the distribution of sorted LEDs when a $60^{\text{o}}$ semi-angle is employed in a randomly located users scenario. As shown in Fig. 2(a), the central LEDs (LED index from 11 to 16) have significantly higher probability of being selected as the best LED for users than the LEDs on the outer circle. Thus, in general, the channel DC gain of one of the central LEDs has an effect on the received power of all of the users. The purpose of activating one of the LEDs on the outside circle will be explained in the next subsection.

*3) Transceiver Algorithm:* In this study, 2-pulse amplitude modulation (PAM) is used for signal shaping. Different DC bias power values, $P_b$, are used to adjust the average transmission power. In the transmission stage, the symbol transmitted to user $k$, $s_k \in [-1, 1]$, is encoded by allocating the power of the activated LEDs. According to the 2-PAM, a simple receiver algorithm can be used to recover the received power. If a threshold value is determined at the receiver side for each user, the recovered data is generated by comparing the received power and the threshold. Thus, before encoding the data vector $\mathbf{s}$, $P_b$ is allocated to all of the activated LEDs to determine the

**Algorithm 1** LED Selection

**Require:** Each user has only one activated LED
**Ensure:** Sum of the activated LEDs is equal to number of the users
**Initialization**;
Sort channel gains of the LEDs on the outer circle in a descend order, sortLEDs $(K \times L)$;
Generate an user index vector $\mathbf{A}$ $(K \times 1)$ with all zero elements;
Generate a power vector $\mathbf{P}$ $(L \times 1)$ with all zero elements;
Set LED index integer to 1, $i \leftarrow 1$;
**while** sum($\mathbf{A}$) $\neq K$ **do**
  Find available LEDs index;
  LEDindex =find($\mathbf{P}$(sortLEDs$(:, i)) = 0$);
  **if** isempty(LEDindex) **then**
    $i \leftarrow i + 1$;
  **else**
    Find user index for available LEDs;
    $k =$ find (sortedLEDs(LEDindex, $i$));
    **if** $A_k = 0$ **then**
      **if** LEDindex is not conflicted among users **then**
        Activate an available LED for each user;
        $P_{\text{LEDindex}} \leftarrow 1$;
        $A_k \leftarrow 1$;
      **else**
        Randomly select one of the conflicted users, $k_l$;
        Activate the conflicted LED for the user $k_l$;
        $P_{\text{LEDindex}} \leftarrow 1$;
        $A_{k_l} \leftarrow 1$;
      **end if**
    **else**
      $i \leftarrow i + 1$;
    **end if**
  **end if**
**end while**
In addition to the activated LEDs, activate all central LEDs;
$P_{11,12,13,14,15,16} \leftarrow 1$.

threshold value $\mathbf{P}_{\text{th}}$ at the receiver:

$$\begin{aligned} \mathbf{P}' &= \mathbf{1} \\ \mathbf{P}_{\text{th}} &= \mathbf{H}' \left(P_b \mathbf{P}'\right). \end{aligned} \tag{11}$$

It is important to note that $\mathbf{P}_{\text{th}}$ is the generated threshold value for users at the transmitter side to allocate power coefficients and, different from (10), the effect of noise is not considered in (11).

After that, depending on the achieved channel gains and the user specific transmitted data, a transmission power of the activated LEDs is allocated by using a search technique as described in Algorithm 2. In Algorithm 2, power coefficients for the activated LEDs are searched to satisfy the threshold constraint of each user according to the transmitted symbol. An interval of [0,2] is used to limit the searching space of the power coefficients. For user $k$, if the transmitted symbol is 1,

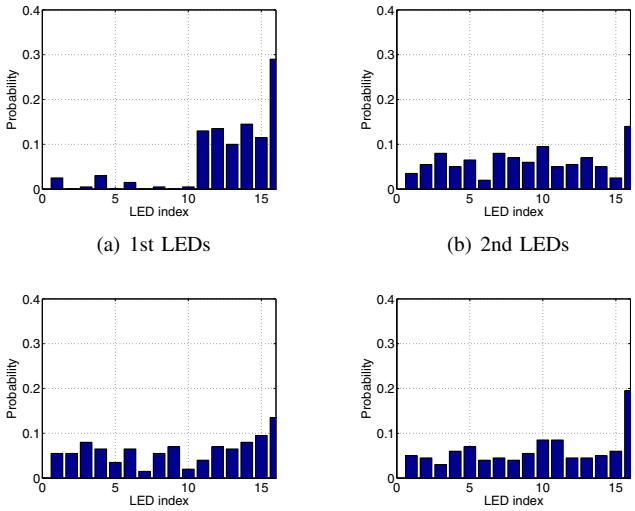


(a) 1st LEDs (b) 2nd LEDs

(c) 3rd LEDs (d) 4th LEDs

Fig. 2. Distribution of sorted LEDs - see Fig. 1 for LED numbering

its received power on the PD should be above its own threshold value $P_{\mathrm{th},k}$. On the other hand, if the transmitted symbol is -1, the received power should be below the threshold of user $k$.

**Algorithm 2** Power Coefficient Search

**Require:** Symbols for users, **S**

**Ensure:** Threshold constraints according to symbol for each user should be satisfied

**Initialization**;

Generate threshold value for each user by using (11);

Generate received power matrix by using possible power coefficient combinations in the interval [0,2]

**for** $k = 1 : K$ **do**

Find possible power coefficients, posCoefs, which satisfies the threshold constraints;

**if** $s_k = 1$ **then**

posCoefs(:,$k$) = find(receivedPower(:,$k$) $>$ $\mathbf{P}_{\mathrm{th}}$(k))

**else**

posCoefs(:,$k$) = find(receivedPower(:,$k$) $<$ $\mathbf{P}_{\mathrm{th}}$(k))

**end if**

**end for**

Find intersection of possible coefficient sets;

$\mathbf{P}' \leftarrow$ posCoefs(:,1) $\cap$ posCoefs(:,2) $\cap \ldots \cap$ posCoefs(:,$K$).

Note that perfect channel knowledge is assumed on the transmitter side. In the proposed transmission strategy, channel information is not required at the receiver side. As noted, before data transmission, the transmitter emits power $P_b$ from all of the activated LEDs and the receiver determines its threshold value by accumulating the received power. After allocating the power of the activated LEDs, data is transmitted and recovered according to the determined threshold value by users:

$$\hat{s_k} = \begin{cases} 1, & y'_k > P_{\mathrm{th},k} + n_k \\ -1, & y'_k < P_{\mathrm{th},k} + n_k \end{cases} \quad (12)$$

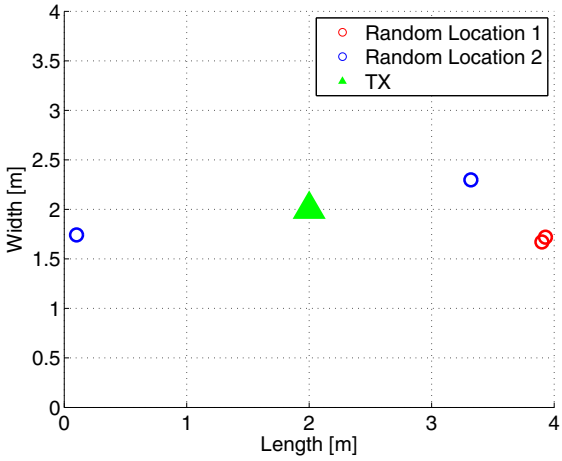


Fig. 3. Random location of users

Fig. 3 shows two different randomly generated user locations when the system has two users. In random location 1, two users are located close to each other and in random location 2, two users are located in an opposite direction from the transmitter. These user locations are employed to explain the power coefficient search algorithm. For simplicity, the power level of the central LEDs is fixed to $P_b$ and only the power coefficients of the activated LEDs on the outer circle are searched. In Fig. 4, the received power and threshold values for users are shown for the scenario involving the random location 1 when the users located close to each other. Inherently, the achieved channel DC gains are similar for these users. Thus, the received power of each user is also similar, as shown by the red and blue points for user 1 and 2 in Fig. 4, respectively. Accordingly, the number of the possible power coefficients that satisfy the given transmitted symbol constraints in Algorithm 2 decreases. However, even for close user locations, there are 10 different possible power coefficients for each different symbol transmission case. In Fig. 4, these coefficients are shown by red and black boxes for transmission of $\mathbf{s} = [-1; 1]$ and $\mathbf{s} = [1; -1]$, respectively. Note that as the power of the central LEDs is fixed, the coefficients are searched in a two dimensional space. When the central LEDs are also taken into account in the searching algorithm, the dimension of the searching space increases to 8 and the number of the possible power coefficients that achieves the given algorithm constraints increases.

In Fig. 5, the received power and possible power coefficients satisfying the given constraints are shown for users located far away from each other (random location 2). When the channel DC gains from the activated LEDs are different for each user, the received power for each user does not overlap, as shown in Fig. 4. For example, when the power coefficient of the activated LEDs for user 1 and 2 are 0.5 and 1.5, the received optical power is approximately around $5 \times 10^{-7}$ W and $10 \times 10^{-7}$ W, respectively. The received power for the same coefficients 0.5 and 1.5 for user 1 and

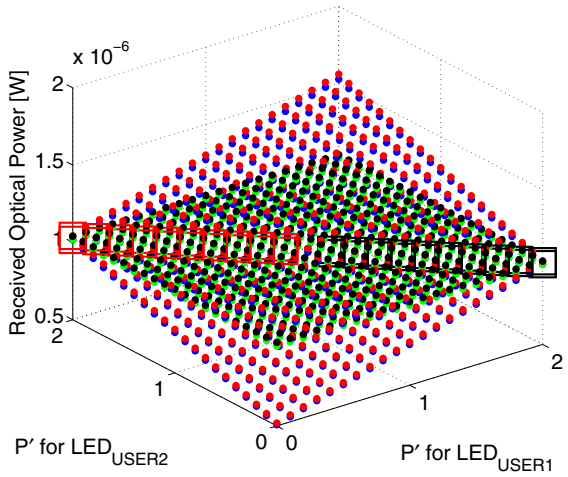


Fig. 4. The received optical power with respect to power coefficients of the selected LEDs for users in 'Random Location 1'. The blue and black points show the received power and threshold for User 1, respectively; the red and green points show the received power and threshold for User 2, respectively; the black and the red squares show the power coefficients that satisfy the constraints for the users when $\mathbf{s} = [1; -1]$ and $\mathbf{s} = [-1; 1]$ is transmitted, respectively.

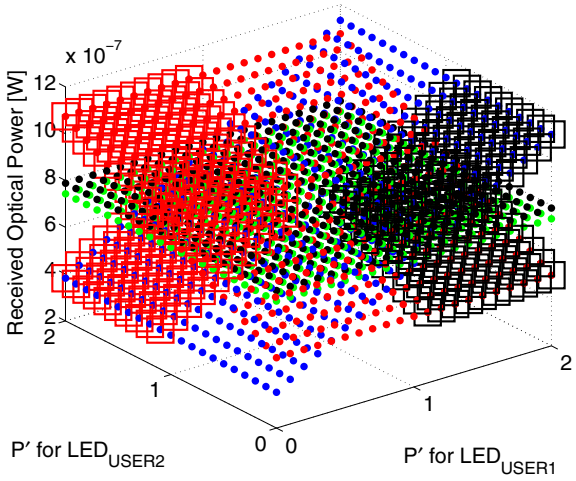


Fig. 5. The received optical power with respect to power coefficients of the selected LEDs for users in 'Random Location 2'. The blue and black points show the received power and threshold for User 1, respectively; the red and green points show the received power and threshold for User 2, respectively; the black and the red squares show the power coefficients that satisfy the constraints for the users when $\mathbf{s} = [1; -1]$ and $\mathbf{s} = [-1; 1]$ is transmitted, respectively.

2, respectively, is around $1 \times 10^{-6}$ W for both users when random location 1 is considered. Accordingly, the number of possible power coefficients that satisfy the constraints are 100 for both $\mathbf{s} = [1; -1]$ and $\mathbf{s} = [-1; 1]$ transmission cases when the random scenario 2 is considered, as shown in Fig. 5.

TABLE I
SIMULATION PARAMETERS

| **Transmitter Parameters** | **Value** |
|---|---|
| Number of LED arrays, $N_t$ | 1 |
| Number of LEDs in a LED array, $L$ | 16 |
| Outer Circle Radius, $R_o$ | 42.5 mm |
| Inner Circle Radius, $R_i$ | 21.25 mm |
| Orientation Angle, $\alpha_{xz}$ | 60° |
| LED Semi-Angle, $\Psi_{\frac{1}{2},T_x}$ | 30°, 60° |
| LED Bias Power - Upper Limit, $P_{b,\text{up}}$ | 20 dBm |
| LED Bias Power - Lower Limit, $P_{b,\text{low}}$ | -40 dBm |
| Power Coefficients Interval | [0,2] |
| **Receiver Parameters** | **Value** |
| Number of PDs at each user, $N_r$ | 1 |
| PD Responsivity, $r$ | 0.4 A/W |
| PD Field-of-View, $\text{FOV}_{R_x}$ | 30°, 60° |
| PD Physical Area, $A_{R_x}$ | 1 cm$^2$ |
| Optical Filter Gain, $G$ | 1 |
| **System Geometry Parameters** | **Value** |
| Transmitter Height | 3 m |
| Receiver Height | 0.75 m |
| Room Dimensions - Length x Width x Height | 4 x 4 x 3 m |
| Reflection Coefficient - Side Wall, $\rho_{\text{wall}}$ | 0.9 |
| Reflection Coefficient - Floor, $\rho_{\text{floor}}$ | 0.2 |
| Reflection Coefficient - Ceiling, $\rho_{\text{ceiling}}$ | 0.8 |
| Wall Division Area, $\Delta A_{n_w}$ | 25 cm$^2$ |
| **System Parameters** | **Value** |
| Bandwidth, $B$ | 50 MHz |
| Number of Users | 2, 4 |
| Pre-Amplifier Noise Density, $i_{\text{amp}}$ | 5x10$^{-12}$ A/Hz$^{-1/2}$ |
| Ambient Light Photocurrent, $\chi_{\text{amp}}$ | 10.93 A/m$^2$/Sr |

## III. SYSTEM SIMULATION

In system simulations, 100 randomly generated user locations are used, and appropriate power coefficients are randomly selected 100 times in each data transmission. Additionally, every possible data set ($2^K$) is iterated $10^3$ times to average BER performance.

### A. Simulation Parameters

The system parameters chosen for the computer simulations are given in Table I. The optical filter gain $G$ is assumed to be 1 and system bandwidth $B$ is assumed to be 50 MHz in all of the simulations. Also, the receiver is assumed to point upwards in all simulations.

### B. Simulation Results

In Fig. 6, the average BER performance of the 60° transmitter semi-angle is shown when 2 and 4 users are deployed in the system. Receiver FOV angles of 30° and 60° are used to show the effect of the physical feature of the PD. A 60° FOV angle has a better average BER performance than the 30° in both user scenarios. The difference between the average transmission power in $10^{-5}$ average BER is 12 dBm and 15 dBm when the 2 and 4 users are deployed, respectively.

The average BER performance is shown in Fig. 7 when a 30° semi-angle is used at the transmitter. The same explanation can be given for the effects of the receiver FOV on the average BER performance in the 60° semi-angle as for the 30°. When a narrow FOV angle is used at the receiver, the 30° semi-angle has worse performance than the 60°. However, when a large FOV angle is used, the 30° semi-angle outperforms

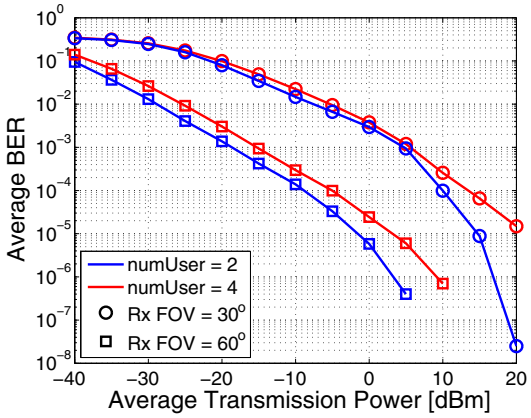


Fig. 6. Average BER performance - $\Psi_{\frac{1}{2},T_x} = 60^{\circ}$

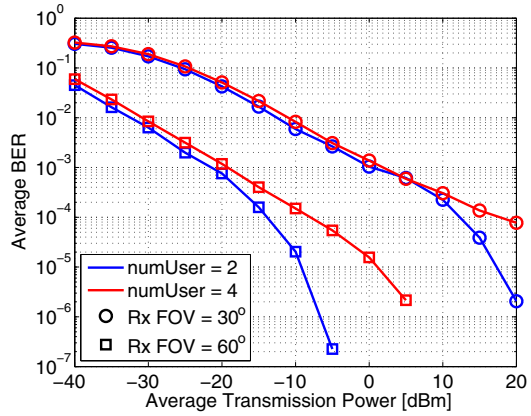


Fig. 7. Average BER performance - $\Psi_{\frac{1}{2},T_x} = 30^{\circ}$

the $60^{\circ}$ semi-angle by 7 dBm and 5 dBm for 2 and 4 users deployment, respectively at the $10^{-5}$ average BER.

The results show an improved average BER performance when using large receiver FOV angle for both $30^{\circ}$ and $60^{\circ}$ semi-angles and this can be explained when the amplitude of the achieved channel DC gains are considered. In general, when a large FOV angle is used, the received power is affected by more activated LEDs. This increases interference and degrades the BER performance when a ZF precoder is used [8]. However, in the proposed transmission strategy, using a large FOV angle increases both the dimensions of the searching space and the number of the possible power coefficients that satisfy the signal transmission constraints. This means that mitigating the interference becomes easier when the transmission power of several LEDs is accumulated at the receiver. In addition to that, using small semi-angles at the transmitter increases the intensity of the optical power in a specific direction. Thus, the difference between the achieved channel DC gains becomes higher. As noted, when users have different channel gains, they also have different received optical power levels, and the number of the possible power coefficients increases, as shown in Fig. 5.

## IV. Conclusions

In this paper, a novel multi-user transmission method is proposed by making use of a compound eye transmitter and the non-negativity characteristic of the transmitted signal in Li-Fi systems. A power allocation approach, based on a LED selection algorithm, is presented instead of precoding at the transmitter which requires finding the inverse or the eigenvectors of the channel. Computer simulation results show that the proposed multi-user transmission method achieves sufficient average BER performance. Future research will focus on designing and optimizing the compound eye transmitter based on the proposed method.

## Acknowledgement

Professor Haas acknowledges support from the Engineering and Physical Sciences Research Council (EPSRC) under the Established Career Fellowship grant EP/K008757/1 and Professor Panayirci acknowledges support from the COST-TUBITAK under the Research grant 113E307.

## References

[1] Ericsson, "Ericsson Mobility Report," Ericsson, Tech. Rep., June 2014.
[2] C.-X. Wang, F. Haider, X. Gao, X.-H. You, Y. Yang, D. Yuan, H. Aggoune, H. Haas, S. Fletcher, and E. Hepsaydir, "Cellular Architecture and Key Technologies for 5G Wireless Communication Networks," *IEEE Commun. Mag.*, vol. 52, no. 2, pp. 122–130, February 2014.
[3] D. Tsonev, S. Videv, and H. Haas, "Light Fidelity (Li-Fi): towards all-optical networking," *Proc. SPIE*, vol. 9007, pp. 900 702–900 702–10, December 2013.
[4] H. Burchardt, N. Serafimovski, D. Tsonev, S. Videv, and H. Haas, "VLC: Beyond Point-to-Point Communication," *IEEE Commun. Mag.*, vol. 52, no. 7, pp. 98–105, July 2014.
[5] K.-H. Park, Y.-C. Ko, and M. Alouini, "On the Power and Offset Allocation for Rate Adaptation of Spatial Multiplexing in Optical Wireless MIMO Channels," *IEEE Trans. Commun.*, vol. 61, no. 4, pp. 1535–1543, April 2013.
[6] Z. Yu, R. Baxley, and G. Zhou, "Multi-User MISO Broadcasting for Indoor Visible Light Communication," *IEEE International Conference on Acoustics, Speech, and Signal Processing (ICASSP)*, pp. 4849–4853, May 2013.
[7] H. Ma, L. Lampe, and S. Hranilovic, "Robust MMSE Linear Precoding for Visible Light Communication Broadcasting Systems," *IEEE Globecom Workshops*, pp. 1081–1086, Dec 2013.
[8] T. Cogalan, H. Haas, and E. Panayirci, "Precoded Single-Cell Multi-User MISO Visible Light Communications," in *Proc. European Wireless Conference, EW2015*, Budapest, Hungary, 20–22 May 2015, (to be published).
[9] J. Zhang, R. Chen, J. Andrews, A. Ghosh, and R. Heath, "Networked MIMO with Clustered Linear Precoding," *IEEE Trans. Wireless Commun.*, vol. 8, no. 4, pp. 1910–1921, April 2009.
[10] M. Joham, W. Utschick, and J. Nossek, "Linear Transmit Processing in MIMO Communications Systems," *IEEE Trans. Signal Processing*, vol. 53, no. 8, pp. 2700–2712, Aug 2005.
[11] K. Karakayali, R. Yates, G. Foschini, and R. Valenzuela, "Optimum Zero-Forcing Beamforming with Per-Antenna Power Constraints," in *IEEE Int. Symp. Inf. Theory, ISIT'07*, June 2007, pp. 101–105.
[12] C. Chen, N. Serafimovski, and H. Haas, "Fractional Frequency Reuse in Optical Wireless Cellular Networks," in *IEEE 24th Int. Symp. on Personal Indoor and Mobile Radio Communications, PIMRC'13*, Sept 2013, pp. 3594–3598.
[13] J. Barry, J. Kahn, W. Krause, E. Lee, and D. Messerschmitt, "Simulation of Multipath Impulse Response for Indoor Wireless Optical Channels," *IEEE J. Select. Areas Commun.*, vol. 11, no. 3, pp. 367–379, Apr 1993.